

SCANNING ELECTRON MICROPROBE CHARACTERIZATION OF AIR FILTERS FROM THE KAVADARCI TOWN AND TIKVEŠ VALLEY

Ivan Boev¹, Tena Šijakova-Ivanova², Dejan Mirakovski³

¹*Faculty of Agriculture, "Goce Delčev" University,
Goce Delčev 89, MK 2000 Štip, Republic of Macedonia*

²*Faculty of Natural and Technical Sciences, "Goce Delčev" University,
P.O. Box 201, MK 2000 Štip, Republic of Macedonia*

³*Faculty of Mechanical Engineering, "Goce Delčev" University,
Goce Delčev 89, MK 2000 Štip, Republic of Macedonia
ivan.boev@ugd.edu.mk*

Abstract: The paper presents data from SEM characterization of Air Filters from Kavadarci town and Tikveš valey, Republic of Macedonia. Several filters from air pumps were submitted for characterization of particulate matter by Scanning Electron Microscopy (SEM) / Energy Dispersive Spectroscopy (EDS). The method of individual particle analysis provides important information about the composition and morphology of the particles, information that otherwise cannot be obtained by bulk analysis methods. The SEM–EDS technique is a valuable tool for the characterization of particles of less than 10 μm (PM₁₀). Additionally, the identification of the morphology and chemical composition of these particles provides valuable information for the determination of their origin. EDS analyses revealed that the filters contained several aluminosilicate phases, including illite, plagioclase, quartz, and possibly amphibole/pyroxene and chlorite. Other phases observed were calcite, gypsum, iron oxides/hydroxides, chromites, silver minerals, and metallic phases. Minor nickel was found associated with metal oxides and stainless steel. No indicated of fibrous materials.

Key words: dust; air filters; Kavadarci town; Tikveš valey

INTRODUCTION

All over the world, air pollution is becoming a major concern. Depending on the conditions, the fine and ultra-fine particulates may persist in the atmosphere for days or weeks and travel hundreds or thousands of miles from their source (Tyagi, 2009). The term dust usually comprises street dust and house dust (Culbard et al. 1988; Fergusson and Kim 1991; Fergusson 1992; Dundar and Ozdemir 2005; Ochsenkühn and Ochsenkühn-Petropoulou 2008).

In 1997 the Environmental Protection Agency (EPA) proposed a new standard of ozone and particulate matter levels in the atmosphere. The particulate matter levels of up to 10 microns in diameter (PM₁₀) at each monitor within an area must not exceed 150 $\mu\text{g}/\text{m}^3$, in one hour more than once per year, averaged over 3 years. The particulate matter

levels of up to 2.5 microns in diameter (PM_{2.5}), must not exceed 15 micrograms per cubic meter ($\mu\text{g}/\text{m}^3$) and 65 $\mu\text{g}/\text{m}^3$, respectively, each year and 24-hour period. Dusts may be classified into natural and synthetic, according to their origin.

Suspended Particulates Matter (SPM) is constituted of aerosol dust or other particulates of size 1 to 200 microns suspended in air (Chandrasekaran et al., 1997).

Mineral dust is mainly constituted of the oxides (SiO₂, Al₂O₃, FeO, Fe₂O₃, CaO, and others) and carbonates (CaCO₃, MgCO₃) that constitute the Earth's crust \pm Global mineral dust emissions are estimated 100–500 millions of tons per year. It is estimated that about 30% of the mineral dust load in the atmosphere could be ascribed to human activities through desertification and land misuse.

Most concerned with dust collection are the mining, metallurgical, coal, gas, iron and steel, clay, chemical, and food industries.

The mineralogical content of dust depends on several conditions: the current erosion of the rocks and soil (Sternik and Goossens, 2007), the traffic intensity in the urban settlements, wind intensity, the presence of the industries generating dust, etc. The quantity of dust in the air as well as its mineralogical

content significantly affect the population health (Ostro, 1994), Poschl (2008) indicated that particle size, chemical composition and mixing states of atmospheric aerosols pose significant impact on climate and human health. Therefore, it is essential to understand size distribution and chemical composition of aerosol particles particularly in urban atmosphere.

METHODOLOGY

The samples were cut and mounted on 25 millimeter Cambridge-style SEM stubs using double sided carbon tape, and graphite coated to prevent charging.

Coated samples were presented to a Quanta 650F SEM, fitted with a back-scattered electron detector (BSED) and a Bruker 5030 X-ray detector.

The Esprit Quantax 1.9 EDS Analysis System was used to determine elemental composition of particulate matter. Point Analysis was used to characterize the samples in high-vacuum mode, using an accelerating voltage of 15 kV and a spot size of 6. BSE images of selected fields of view were taken to examine SEM-based characteristics.

RESULTS

EDS analyses revealed that the filters contained several aluminosilicate phases, including quartz, illite, plagioclase, and possibly amphibole/pyroxene and chlorite.

SiO₂ particles (commonly called silica) are characterized by high content Si and O. Silica was observed in sample 11.

The pure silica particles have natural and anthropogenic origins (Liet *al.*, 2010b). These particles have tubular structure. It is the most abundant chemical constituent of Earth's crust and a major component of sandstone and granite. Thus, the most abundant source for this particle type is soil related. Additionally, silica is widely used for making building materials.

Aluminosilicate particles are composed primarily of feldspar (Si, Al, Ca or Si, Al, Na) and clay (Si, Al or Si, Al, Fe), their origin is mainly crustal, but they can also come from erosion of building products and road dust. Other elements are present in minor concentration in the aluminosilicate particles. These particles mainly present an angular shape, ranging from polyhedral to sharp one. Illite and plagioclase were identified in sample 4 (Fig. 1). Chemical composition of these minerals is shown in Tables 1 and 2, respectively.

Figure 1 showing illite, plagioclase and spores or pollen. EDS spectra of illite and plagioclase are given on Figs. 2A and 2B.

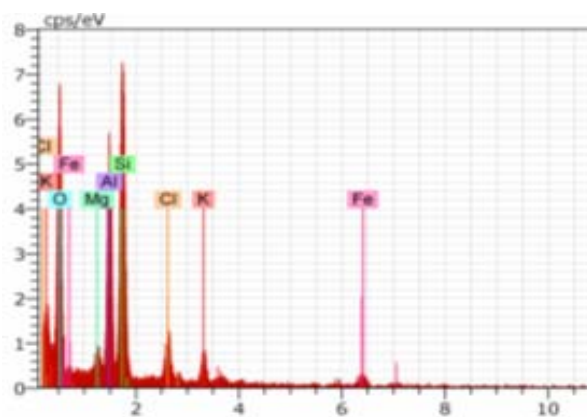


Fig. 2A. EDS spectrum of illite

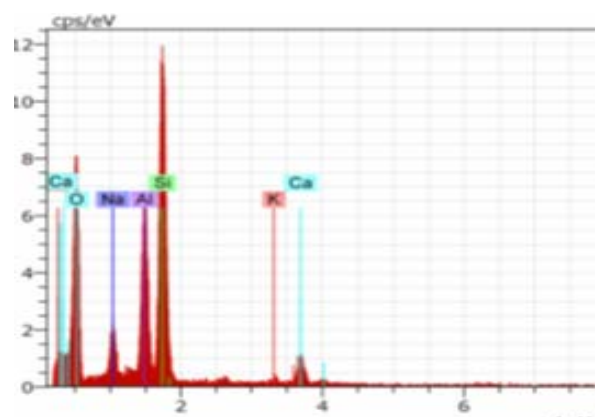


Fig. 2B. EDS spectrum of plagioclase

Table 1

Chemistry of Illite

El	AN	Unn. c. (mass %)	Norm. c. (mass %)	Atom. c. (At %)
O	8	46.26	52.32	67.71
Mg	12	1.83	2.07	1.77
Al	13	11.17	12.64	9.70
Si	14	17.38	19.65	14.49
Cl	17	3.52	3.98	2.32
K	19	3.06	3.47	1.84
Fe	26	5.19	5.87	2.18
Total		88.4%		

Table 2

Chemistry of plagioclase

El	AN	Unn. c. (mass%)	Norm. c. (mass%)	Atom. c. (At%)
O	8	46.51	46.09	59.95
Na	11	5.99	5.93	5.37
Al	13	14.26	14.14	10.90
Si	14	28.20	27.94	20.70
K	19	0.90	0.85	0.47
Ca	20	5.05	5.00	2.60
Total		100.9%		

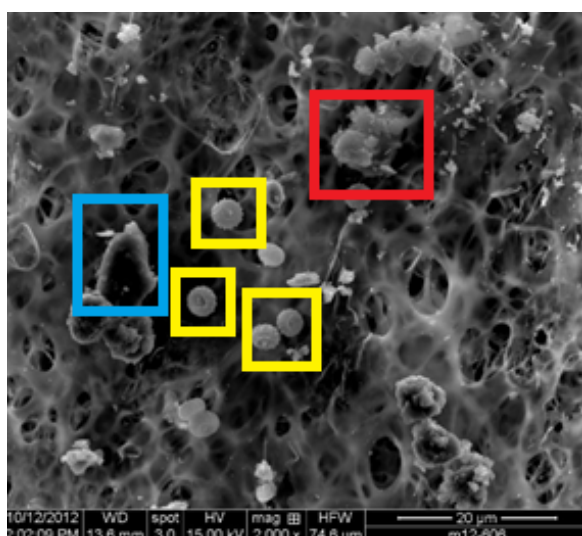


Fig. 1. BSE image of Sample 4 showing illite (red), plagioclase (blue), and spores or pollen (yellow).

Calcium rich particles

Particles composed of high content of Ca (<50% relative contribution by weight) fall into this group. Carbonate minerals identified include calcite (CaCO_3) along with traces of other dust-related elements which are the common constituent of soil and often observed in the individual aerosol particle analysis (Lu *et al.*, 2006; Shao *et al.*, 2008). These particles are irregular fragments with distinct rough surfaces on all faces originated from process of building construction and demolition and commonly found in Earth's crust. The morphology of this small particle suggests its mineral origin.

Calcium carbonate was observed on and around clay minerals in sample 4. (Fig. 3).

Chemistry of calcium carbonate is given in Table 3 and 4.

Table 3

Chemistry of calcium carbonate around aluminosilicates

El	AN	Unn. c. (mass%)	Norm. c. (mass%)	Atom. c. (At%)
O	8	38.41	52.22	69.07
Mg	12	2.21	3.00	2.61
Al	13	6.20	8.44	6.62
Si	14	11.84	16.09	12.12
Cl	17	0.53	0.72	0.43
K	19	1.30	1.77	0.96
Ca	20	7.23	9.83	5.19
Fe	26	5.83	7.93	3.01
Total		73.6%		

Table 4

Chemistry of calcium carbonate on aluminosilicates

El	AN	Unn. c. (mass%)	Norm. c. (mass%)	Atom. c. (At%)
C	6	14.23	14.31	24.65
O	8	38.72	38.93	50.36
Mg	12	0.43	0.43	0.37
Al	13	1.02	1.03	0.79
Si	14	1.79	1.80	1.32
Cl	17	0.56	0.56	0.33
Ca	20	42.71	42.94	22.18
Total		99.5%		

Manganochromite and stainless steel were observed in sample 4. Figure 4A shows BSE images of Manganochromite while Figure 4B shows EDS spectra of manganochromite. BSE images and EDS spectra of stainless steel is shown in Figures 4C and D respectively.

Metals, metal oxides, and metal oxyhydroxides were found with clay minerals. BSE images and EDS spectra are given in Figures 4E and 4F, respectively.

Minor nickel was found associated with metal oxides and stainless steel (Fig. 4D).

Also, metals, metal oxides, and metal oxyhydroxides were found with clay minerals (Fig. 5).

Hydrous phases, observed to be volatile under the electron beam, presumably produced water vapour or carbon dioxide as an effect of heating (Fig. 5 E, F.)

Minor nickel was found associated with metal oxides (Fig. 5B),

The filter contained carbon and chlorine, which may be present as background in mineral spectra. Sample 11 also contained several, relatively large, carbon rich globules.

Carbon-rich particles: The group with the highest abundance corresponds to that of carbon-rich particles mainly from natural origin. Carbon-rich particles of natural origin are pollen and spores. Additionally, spheroidal particles associated with sulfur in some of their edges were observed, possibly due to adsorption and the formation of secondary phases from SO_4^{-2} present in the environment.

Several (alumino)silicates with varying elemental compositions could not be conclusively identified (e.g., Fig. 6). Chemistry of iron magnesium silicate and iron magnesium aluminosilicate is given in Tables 5 and 6, respectively.



Fig. 3A)

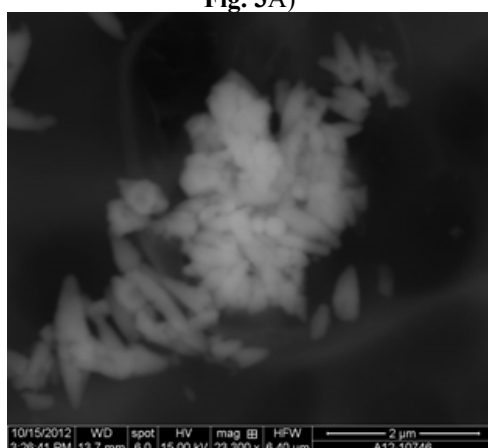


Fig. 3C)

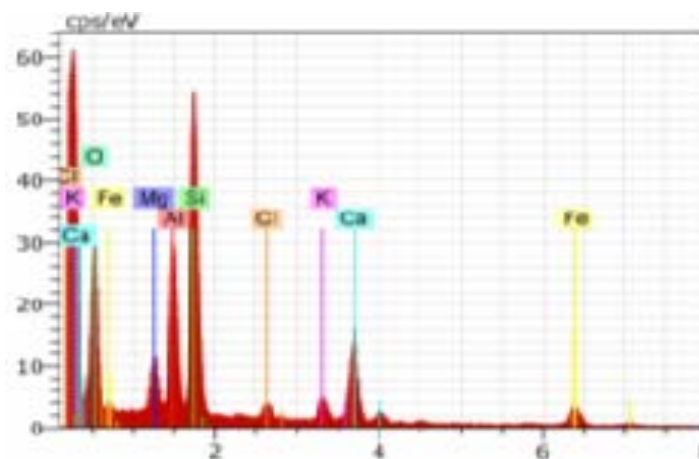


Fig. 3B)

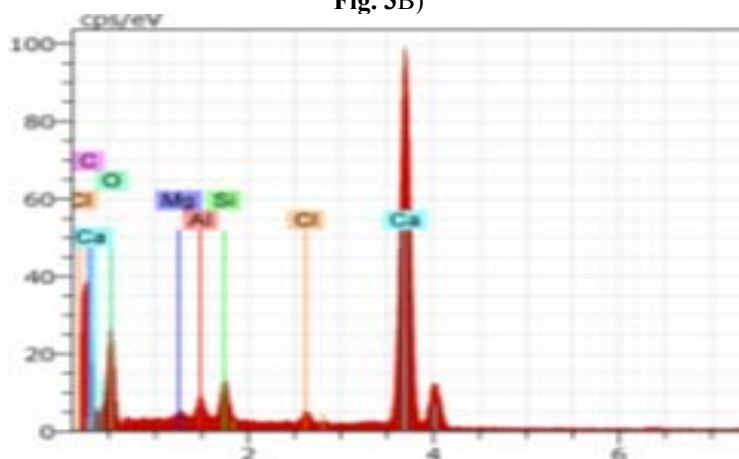


Fig. 3D)

Fig. 3. BSE images and EDS spectra of sample 4.

A) BSE images of calcium carbonate (indicated in A) around aluminosilicates; B) EDS spectra of calcium carbonate around aluminosilicates; C) BSE images of calcium carbonate on aluminosilicates; D) EDS spectra of calcium carbonate on aluminosilicates

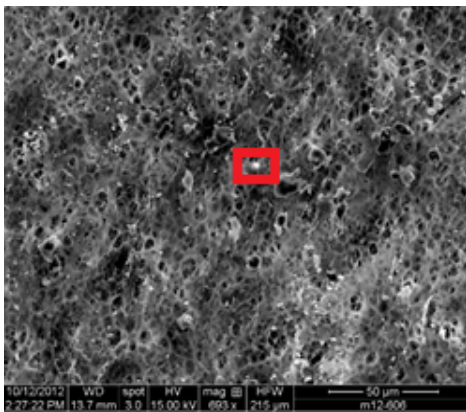


Fig. 4A)

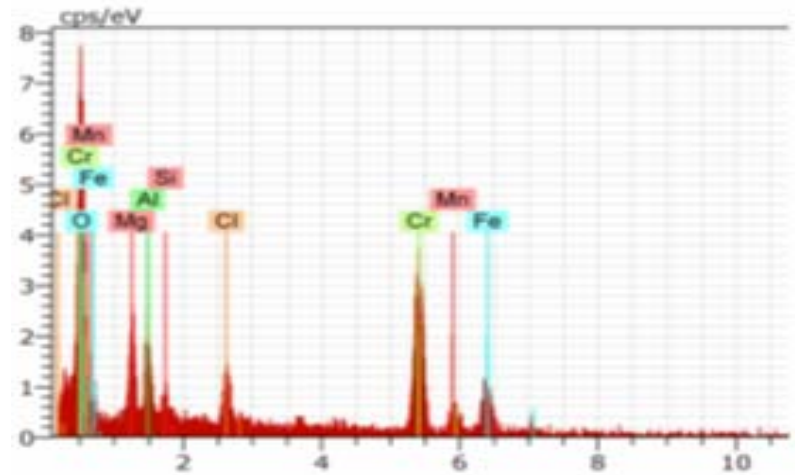


Fig. 4B)

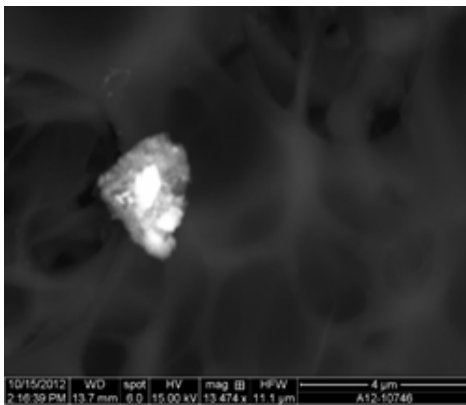


Fig. 4C)

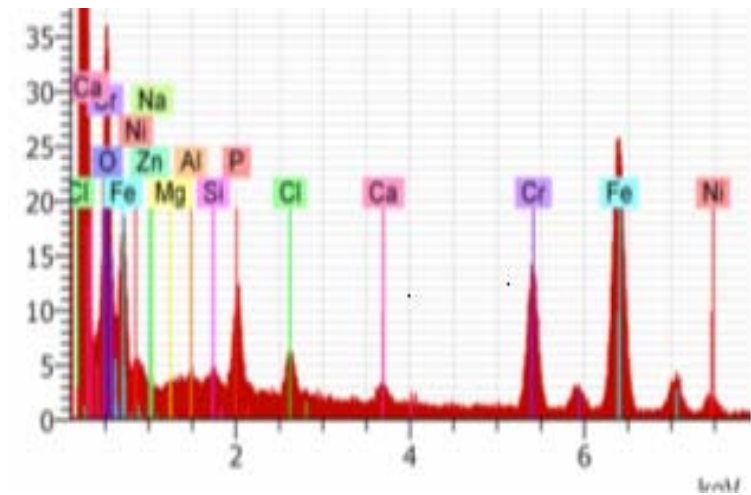


Fig. 4D)

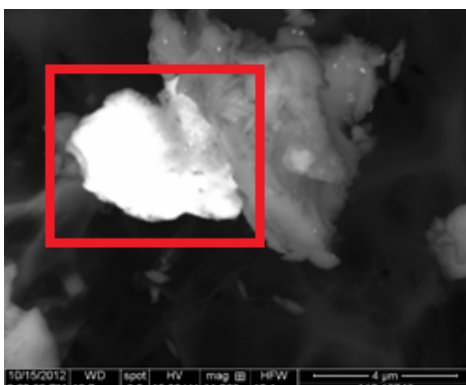


Fig. 4E)

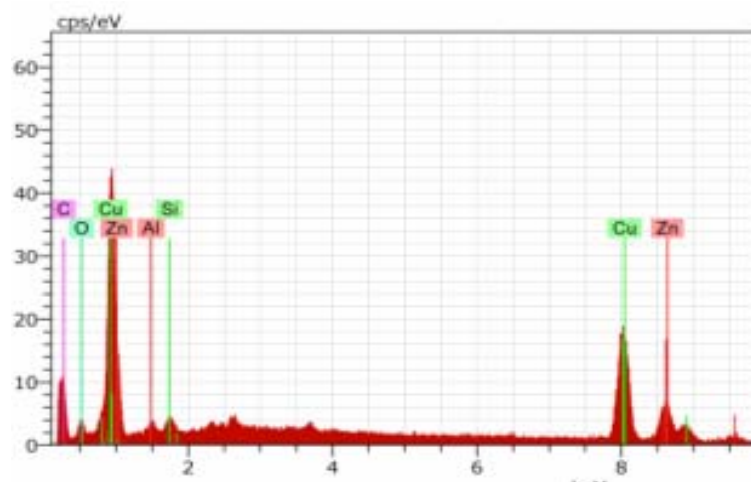


Fig. 4F)

Fig. 4. BSE images and EDS spectra of metallic phases in Sample 4.

A, B) Manganochromite (indicated in A) C; D) corrosion resistant stainless steel; E, F) metallic copper, zinc coating (indicated in E) on a sodium, magnesium aluminosilicate

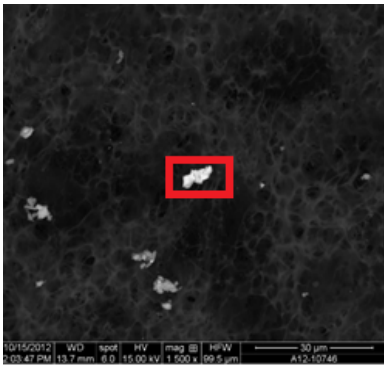


Fig. 5A)

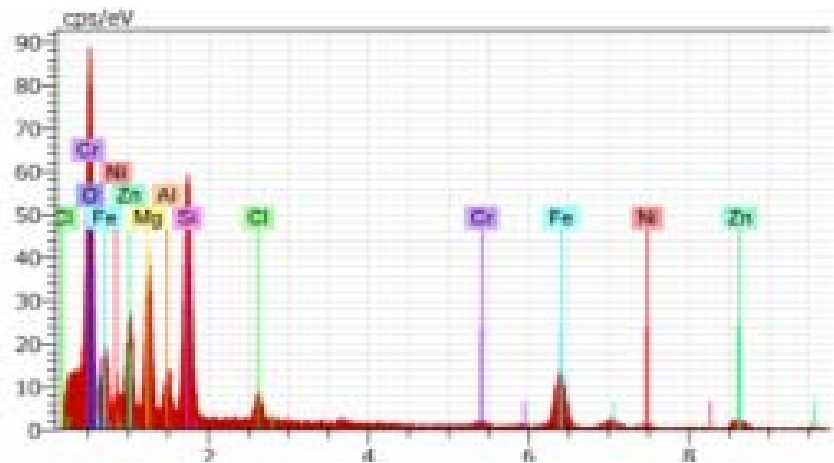


Fig. 5B)

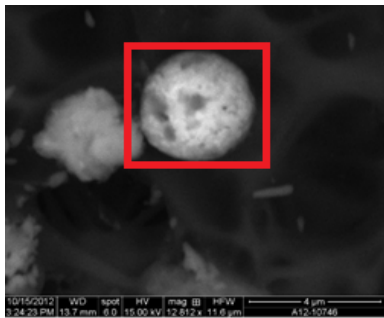


Fig. 5C)

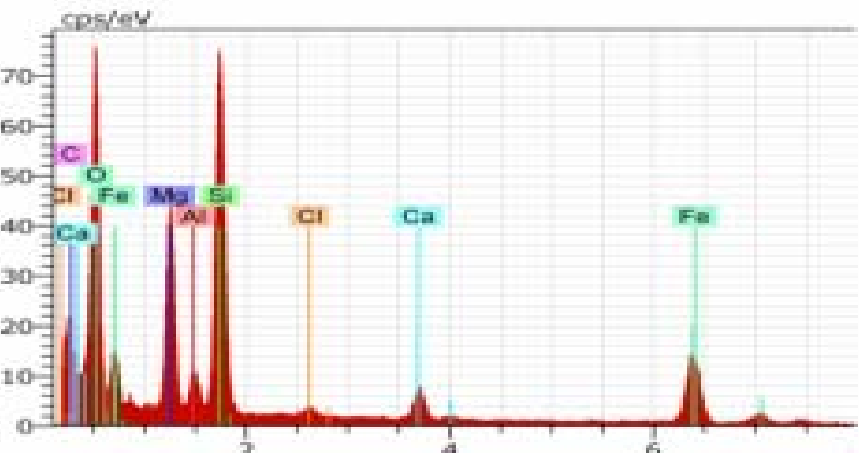


Fig. 5D)

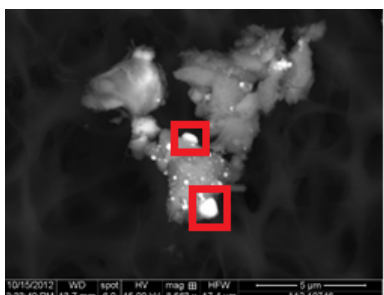


Fig. 5E)

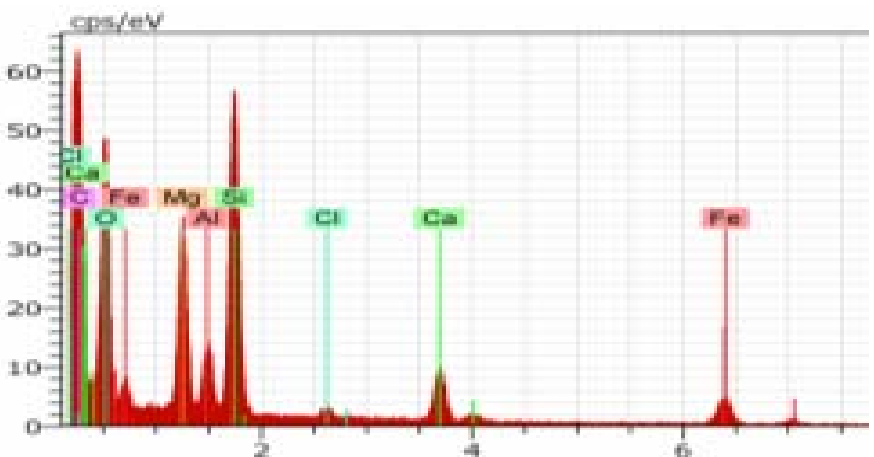


Fig. 5F)

Fig. 5. BSE images and EDS spectra of oxides in Sample 4.
 A, B) Magnesium silicate with metal oxide (indicated in A); C, D) iron oxide on a magnesium silicate (possibly pyroxene/amphibole) (indicated in C); E, F) iron oxyhydroxides (indicated in E) on a hydrated magnesium clay mineral

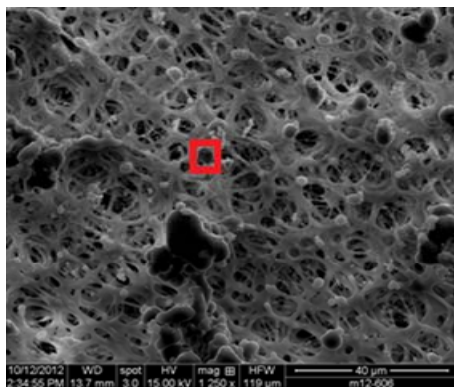


Fig. 6A)

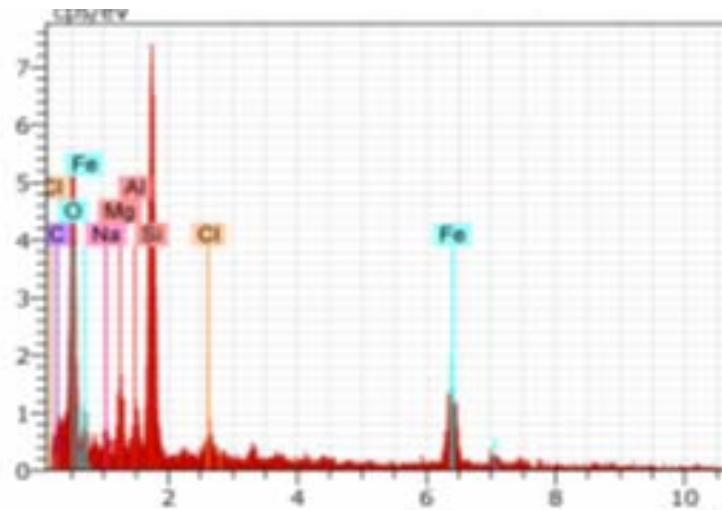


Fig. 6B)

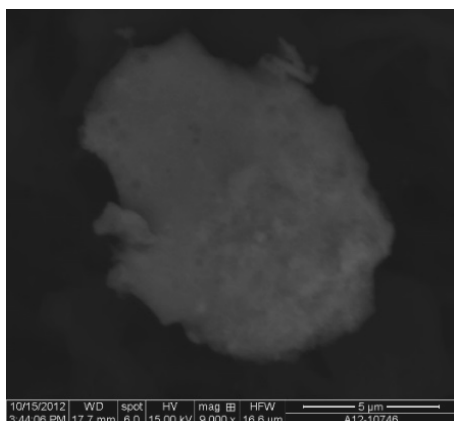


Fig. 6C)

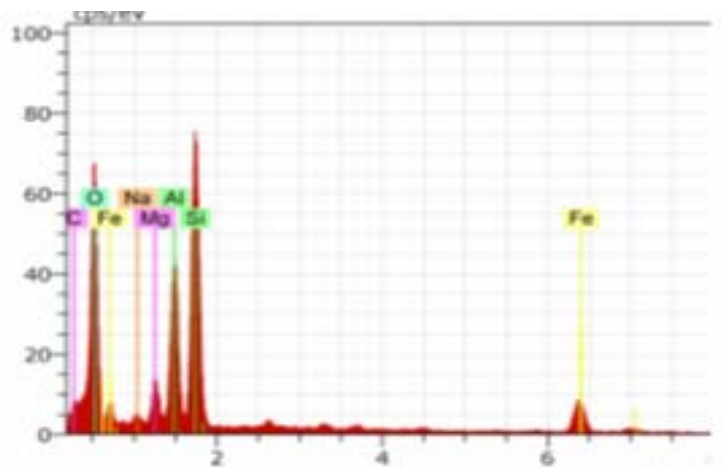


Fig. 6D)

Fig. 5. BSE images and EDS spectra of Sample 11. A, B) Iron magnesium silicate (indicated in A); C, D) Iron magnesium aluminosilicate (possibly chlorite)

Table 5

Chemistry of iron magnesium silicate

El	AN	Unn. c. (mass%)	Norm. c. (mass%)	Atom. c. (At%)
C	6	6.67	8.16	15.12
O	8	30.89	37.78	52.58
Na	11	1.57	1.92	1.86
Mg	12	2.59	3.16	2.90
Al	13	1.65	2.01	1.66
Si	14	14.05	17.19	13.63
Cl	17	1.33	1.63	1.02
Fe	26	23.01	28.15	11.22
Total		81.8%		

Table 6

Chemistry of iron magnesium aluminosilicate (possibly chlorite)

El	AN	Unn. c. (mass%)	Norm. c. (mass%)	Atom. C. (At%)
C	6	7.83	8.03	13.55
O	8	44.82	45.97	58.24
Na	11	0.96	0.99	0.87
Mg	12	2.62	2.69	2.24
Al	13	9.15	9.38	7.05
Si	14	16.58	17.00	12.27
Fe	26	15.53	15.93	5.78
Total		97.5%		

Calcium sulfate – these particles are originated by acid-base neutralization reactions in atmosphere and by deterioration of building's surface, composed of CaCO_3 (marble and limestone), and it is due to reaction with sulfur compounds in the atmosphere. Calcium sulfate is also used for the production of cement and it is a secondary product of desulphurization of flue gas. The shape of these particles is typically symmetrical and elongated, even if there are irregular examples of particles, too.

Gypsum was observed in sample 11 (Figs. 7A, B). Metals, metal oxides, and metal oxyhydroxides were found with clay minerals (Figs. 7C, D).

Hydrous phases, observed to be volatile under the electron beam, presumably produced water vapour or carbon dioxide as an effect of heating (Figs. 7C, D).

The chemistry of gypsum is shown in Table 7, while the chemistry of iron oxides/oxyhydroxides is shown in Table 8.

Silver and associated minerals were observed in sample 11 (Fig. 8).

Chlorargyrite (Figs. 8A, B), with minor acanthite. Chlorargyrite and silver (bright phase indicated in C) (Figs. 8C, D). Silver mineral (Figs. 8E, F), can be of crustal origin, but may also come from human activities such as industrial processes.

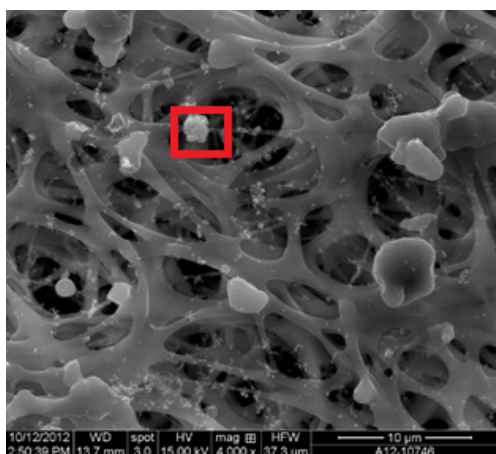


Fig. 7A)

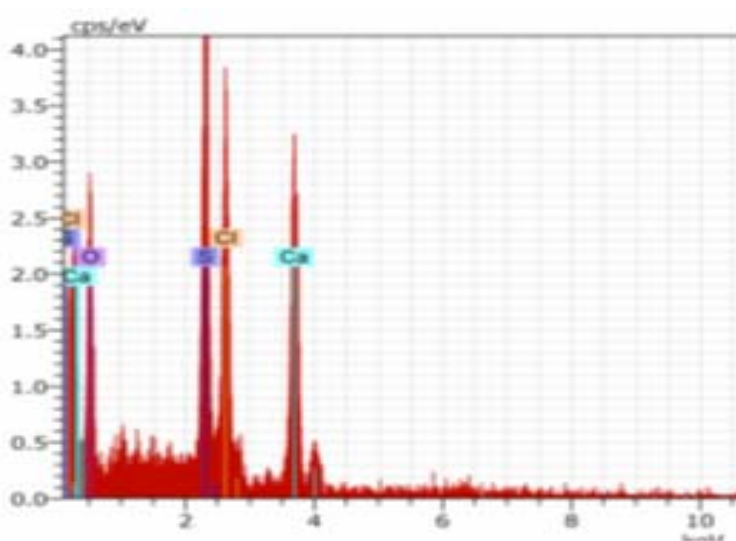


Fig. 7B)

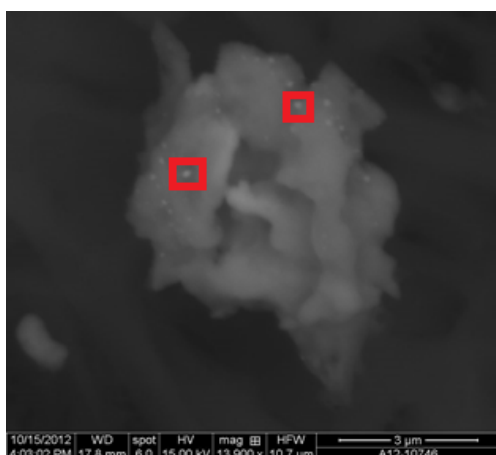


Fig. 7C)

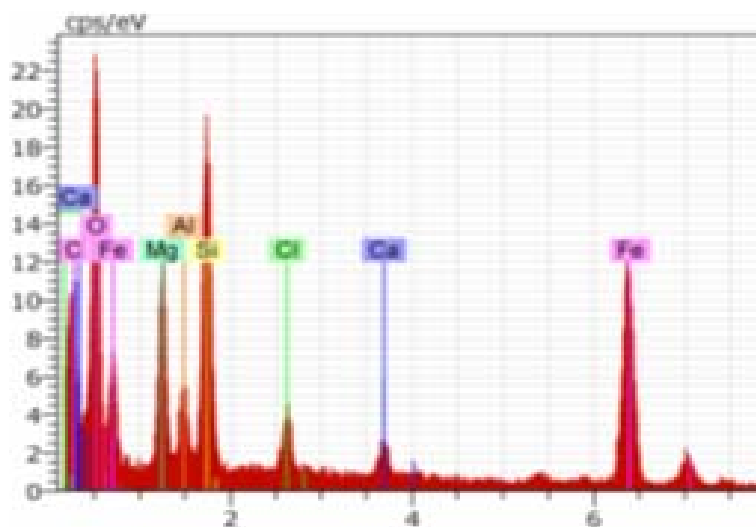


Fig. 7D)

Fig. 7. BSE images and EDS spectra of Sample 11.

A, B) Gypsum (indicated in A); C, D) iron oxides/oxyhydroxides (indicated in C) on a magnesium silicate mineral.

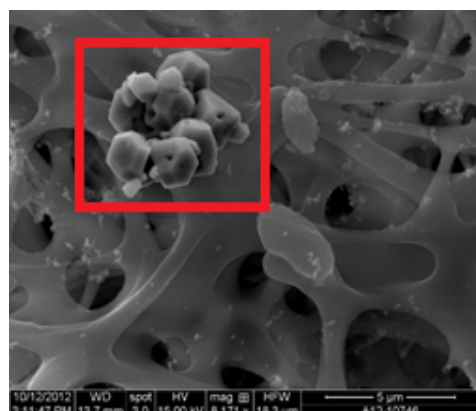


Fig. 8A)

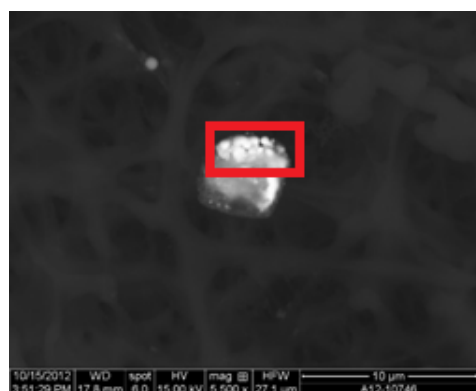
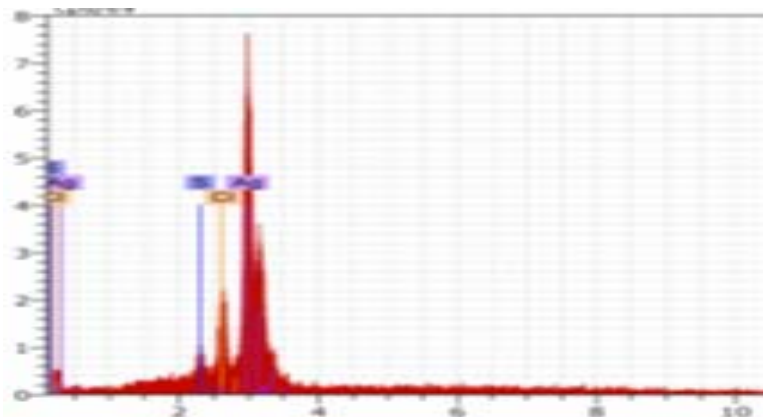


Fig. 8C)

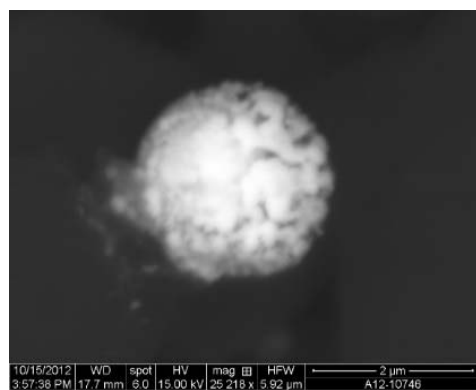
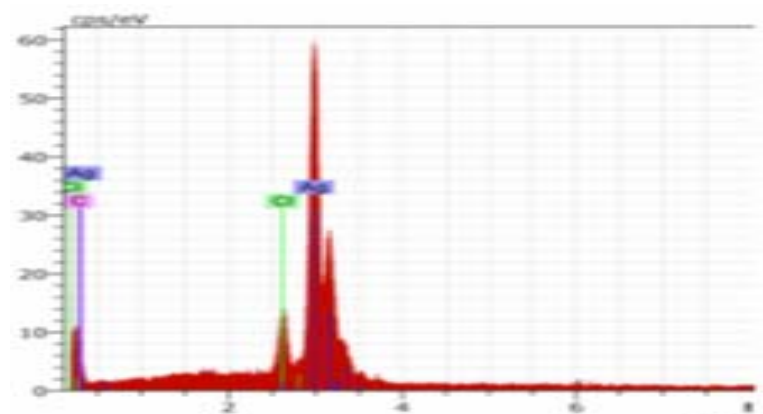


Fig. 8E)

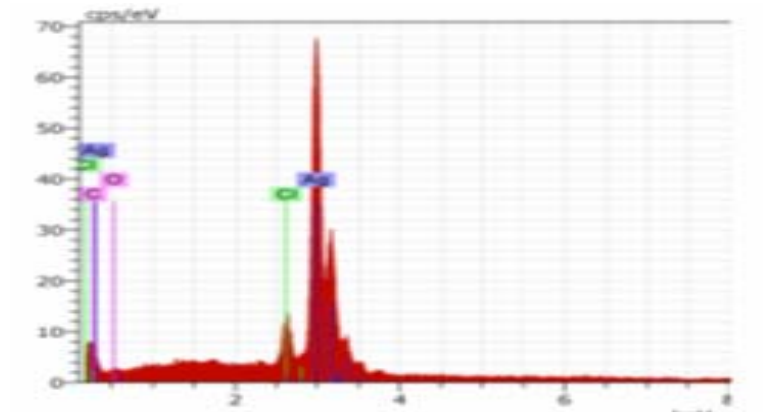


Fig. 8. BSE images and EDS spectra of silver minerals in Sample 11.

A, B) Chlorargyrite (indicated in A) with minor acanthite (seen in B); C, D) Chlorargyrite and silver (bright phase indicated in C).
E, F) Silver mineral.

In aerosol of this region also have been identified: metal oxides and sulfides; magnesium silicate with iron oxide (Fig. 9A, B); magnesium silicate with zinc, iron oxide (Fig. 9C, D); and aluminosilicate coated by iron, chromium, titanium and nickel oxides and/or sulfide (Fig. 9E, F). This group of particles mainly corresponds to Fe oxides with irregular morphology which are assumed to be soil related.

Minor nickel was found associated with metal oxides (Fig. 8E). Metals, metaloxides, and metal oxyhydroxides were found with clay minerals (Fig. 8).

Because these minerals are present in the ore processed in the ferronickel smelter plant which is situated in this area, we can conclude that the content of these particles in the analyzed samples come from human activities in the metallurgical plant.

Table 7

Chemistry of gypsum

El	AN	Unn. c (mass%)	Norm. c (mass%)	Atom. c (At%)
O	8	41.08	54.65	73.16
S	16	9.84	12.79	8.54
Cl	17	9.90	12.86	7.77
Ca	20	15.17	19.70	10.53
Total		77%		

Table 8

Chemistry of iron oxides/oxyhydroxides (indicated in C) on a magnesium silicate mineral

El	AN	Unn. c (mass%)	Norm. c (mass%)	Atom. c (At%)
C	6	7.29	7.98	17.73
O	8	21.39	23.41	39.03
Mg	12	5.94	6.50	7.14
Al	13	2.18	2.39	2.36
Si	14	8.62	9.43	8.96
Cl	17	1.45	1.59	1.20
Ca	20	1.55	1.70	1.13
Fe	26	42.96	47.01	22.46
Total		91.4%		

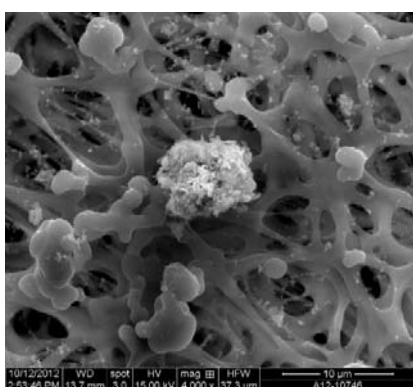


Fig. 9A)

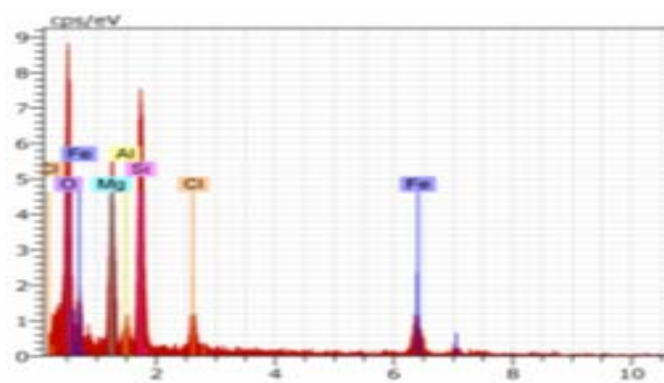


Fig. 9B)

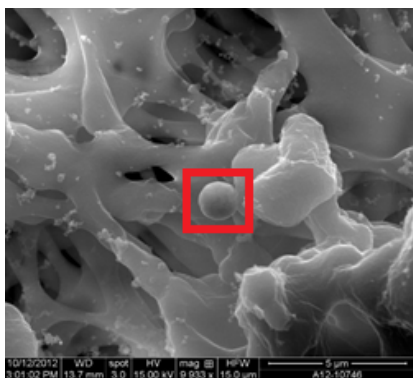


Fig. 9C)

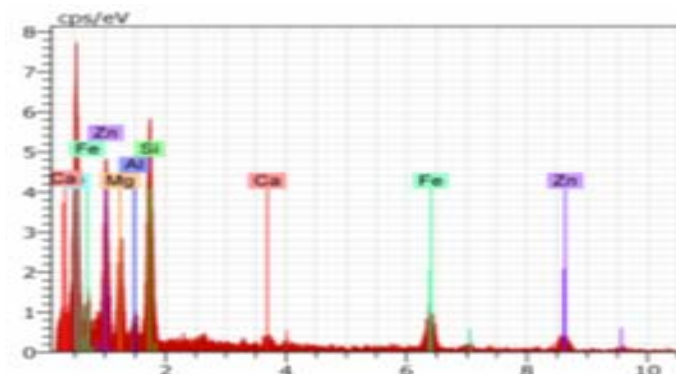
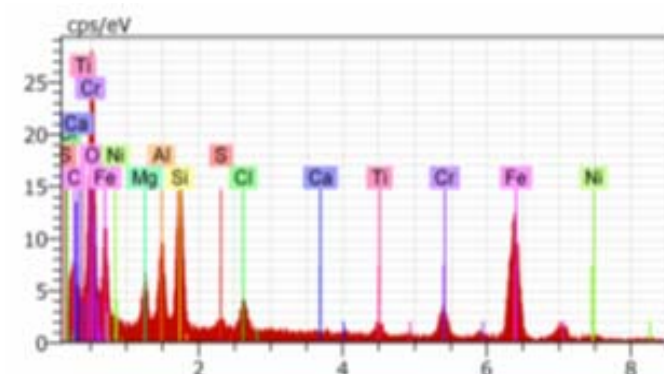


Fig. 9D)



E)



F)

Fig. 9. BSE images and EDS spectra of metal oxides and sulfides in Sample 11.

A, B) Magnesium silicate with iron oxide. C, D) Magnesium silicate with zinc, iron oxide (indicated in C).

E, F) Aluminosilicate coated by iron, chromium, titanium and nickel oxides and/or sulfides

CONCLUSION

Based on investigations carried out it can be inferred the following:

Filters contained several aluminosilicate phases, including illite, plagioclase, quartz, and possibly amphibole/pyroxene and chlorite. Other phases observed were calcite, gypsum, iron oxides/hydroxides, chromite, silver minerals, and metallic phases. Minor nickel was found associated

with metal oxides and stainless steel. No indication of fibrous materials

Particles such as illite, plagioclase, quartz, amphibole/pyroxene, chlorite, calcite and gypsum are mainly from natural origin, while iron oxides / hydroxides, chromite, silver minerals and nickel come from human activities such as industrial processes, especially the ferronickel smelter plant which is situated in this area.

REFERENCES

- [1] Culbard E. B, Thornton I., Watt J., Wheatley M., Moorcroft S., Thompson M. (1988): Metal contamination in British urban dusts and soils. *J. Environ. Qual.*, **17**, 226–234.
- [2] Chandrasekaran, G. E., Ramchandran, C., Shetty, N. (1997): Ambient air quality at selected sites in Bangalore City, *Indian Journal of Environmental Production*, **17**, 184–188.
- [3] Dundar M. S., Ozdemir F. (2005): Heavy metal contents of indoor air dust particulate matter from Adapazari, Turkey. *Fresen. Environ. Bull.*, **14**, 189–193.
- [4] Fergusson J. E., Kim N. D. (1991): Trace elements in street and housedusts: source and speciation. *Sci. Total Environ.*, **100**, 125–150.
- [5] Fergusson J. E. (1992): In: Dunnette D. A., O'Brien R. J. (ed.). *The science of global change, the impact of human activities on the environment*. American Chemical Society, Washington, pp. 116–133.
- [6] Li, W., Shao, L. Y., Shen, R., Wang, Z., Yang, S., Tang, U. (2010b): Size, Composition and Mixing State of individual Aerosol Particles in South China Coastal City. *J. Environ. Sci.* **22**, 561–569.
- [7] Lu, S. L., Shao, L. Y., Wu, M. H., Jiao, Z. (2006): Mineralogical Characterization of Airborne Individual Particulates in Beijing PM10. *J. Environ. Sci.* **18**, 90–95.
- [9] Ochsenkühn K-M., Ochsenkühn-Petropoulou M. (2008): Heavy metals in airborne particulate matter of an industrial area in Attica, Greece, and their possible sources. *Fresen. Environ. Bull.*, **17**, 455–462.
- [9] Ostro B. (1994): Estimating the health effects of air pollutants: A method with an application to Jakarta. *Policy Research Working Paper 1301*. World Bank, Policy Research Department, Washington, DC.
- [10] Poschl, U. (2005): Atmospheric Aerosols: Composition, Transformation, Climate and Health Effects. *Angew. Chem. Int. Ed.* **44**. 7520–7540.
- [11] Sterk G., Goossens D. (2007): Emissions of soil dust and related problems in Europe: An overview. *Proceeding on Dust Conference 2007: How to Improve Air Quality*, Maastricht, April 23–24, 2007.
- [12] Tyagi, S. K. (2009): A need for in-depth studies of airborne particle size distribution in Delhi formulation of ambient air standard for PM2.5, *Indian Journal of Air Pollution Control*, **9**, 22–26, 2009.

Резиме

ЕЛЕКТРОНСКА МИКРОАНАЛИЗА НА ВОЗДУШНИ ФИЛТРИ ОД ГРАДОТ КАВАДАРЦИ И ТИКВЕШКАТА ДОЛИНА

Иван Боев¹, Тена Шијакова-Иванова², Дејан Миравовски³

¹Земјоделски факултет, Универзитет „Гоце Делчев“, Гоце Делчев 89, МК 2000 ШТИИ, Република Македонија

²Факултет за природни и технички науки, Универзитет „Гоце Делчев“, п. фах 201, МК 2000 ШТИИ, Република Македонија

³Машински факултет, Универзитет „Гоце Делчев“, Гоце Делчев 89, МК 2000 ШТИИ, Република Македонија
ivan.boev@ugd.edu.mk

Клучни зборови: прав; воздушни филтри; Кавадарци; тиквешки регион

Во овој труд се презентирани податоци од испитувањата на прав од воздушни филтри со методот на СЕМ/ЕДС (сканинг електронска микроскопија / енергетски дисперзивна спектроскопија). Ваквиот начина на анализирање на индивидуални честички дава значајни инфор-

мации за составот и морфологијата на честичките, кои не можат да се добијат со другите аналитички методи.

Со овој метод е испитан праот од неколку воздушни филтри од градот Кавадарци и тиквешката околина.

Од добиените податоци може да се види дека правот од филтрите се состои од неколку алумосиликатни фази, вклучувајќи илит, плагиоклас, кварц, амфиболи или пироксени и хлорит. Од другите фази се застапени калцит, гипс, железени оксиди / хидроксида, хромит, минерали на

сребро и металични фази. Мала концентрација на никел е најдена во асоцијација со металните оксиди и не'ргосувачки челик. Присуство на влакнести минерали не е утврдено.